

## Views

Rudolf Weber\* and Thomas Graf

# The challenges of productive materials processing with ultrafast lasers

<https://doi.org/10.1515/aot-2021-0038>

Received August 16, 2021; accepted September 21, 2021;  
published online October 14, 2021

**Abstract:** Materials processing with ultrafast lasers with pulse durations in the range between about 100 fs and 10 ps enable very promising and emerging high-tech applications. Moreover, the average power of such lasers is steadily increasing; multi kilowatt systems have been demonstrated in laboratories and will be ready for the market in the next few years, allowing a significantly increase in productivity. However, the implementation of ultrafast laser processes in applications is very challenging due to fundamental physical limitations. In this paper, the main limitations will be discussed. These include limitations resulting from the physical material properties such as the ablation depth and the optimal fluence, from processing parameters such as air-breakdown and heat accumulation, from the processing system such as thermal focus shift, and from legal regulations due to the potential emission of soft X-rays.

**Keywords:** ablation efficiency; air-breakdown; heat accumulation; soft X-ray emission; thermal lens; ultrafast laser materials processing.

## 1 Introduction

In the year 2013 materials processing with ultrafast lasers with pulse durations in the range between about 100 fs and 10 ps won the “Deutscher Zukunftspreis” as a very promising high-tech application. While the “industry-standard” average power of commercial ultrafast lasers was in the range of 50 W at that time, the potential of the technology was impressively confirmed by the first demonstration of

an ultrafast laser delivering an average power exceeding 1 kW with pulse energies exceeding 1 mJ by Negel et al. [1] in the same year. The increase of the average power of ultrafast lasers over the years is shown in Figure 1. The dark blue squares represent the maximum average power achieved in research laboratories at that time, the light blue squares refer to the lasers of this kind that are explicitly mentioned in this text. The green triangles represent average powers of typical commercially available ultrafast laser systems for industrial applications. Two further milestones have recently corroborated the ongoing rapid development of this technology.

In 2017, Nubbemeyer et al. [3] presented a 1 ps-laser with an average power of 1 kW and a pulse energy of 200 mJ, which is almost four orders of magnitude (!) larger than that of actual industrial lasers. Last year, an average power exceeding 10 kW was demonstrated by Müller et al. [4].

It can be concluded that the average power of ultrafast lasers is subject to a kind of Moor’s law: the average power of these lasers doubles every three years and there is no limit in sight yet. Furthermore, it can be seen that the average power attained by the lasers in research laboratories precedes the average power of standard industrial lasers by about 10 years. This means, that ultrafast lasers with an average power of 10 kW will be an industry standard in the year 2030.

Today, materials processing with ultrafast lasers are still regarded as an emerging and very promising technology. This aptly describes the fact that only a few processes are established in industrial large-scale applications, such as in particular cutting of glass, which is used for example to shape the displays of smartphones, and that we are still far from having fully tapped the potential of this technology. Ablative processes such as microcutting, drilling of precise and deep holes, or “laser-turning” of rotationally symmetrical shapes allow successful niche-applications but presently run at moderate average powers of a few tens of Watts. One of the reasons for the still limited market penetration of the ultrafast laser technology is that almost every application needs the development of a tailored process. This complicates cost reduction through quantity.

\*Corresponding author: Rudolf Weber, Institut für Strahlwerkzeuge, Universität Stuttgart, Pfaffenwaldring 43, D-70569 Stuttgart, Germany, E-mail: rudolf.weber@ifsw.uni-stuttgart.de  
Thomas Graf, Institut für Strahlwerkzeuge, Universität Stuttgart, Pfaffenwaldring 43, D-70569 Stuttgart, Germany

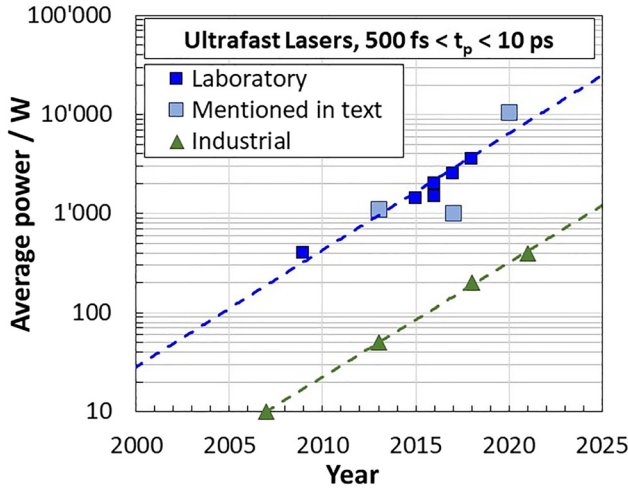


**Figure 1:** Evolution of the average power of ultrafast lasers, see e.g. [2]. The dark blue squares represent the maximum average power achieved in research laboratories at that time, the light blue squares refer to the lasers of this kind that are explicitly mentioned in this text. The green triangles represent average powers of typical commercially available ultrafast laser systems for industrial applications.

However, the biggest challenge today is to scale the productivity of ultrafast laser applications. The productivity of laser processes can be expressed by the volume of the material which is processed per unit time, given by

$$\dot{V} = \frac{\eta_p}{h_V} \cdot P_{av}, \quad (1)$$

where  $\eta_p$  is the overall process efficiency (considering absorption and thermal losses),  $h_V$  is the volume-specific energy, which is required for the particular process in the given material, and  $P_{av}$  is the average laser power. This simple equation states that the productivity  $\dot{V}$  essentially only depends on the material and linearly scales with the average laser power, when the process efficiency (which, among others, depends on the applied fluence, see below) is kept constant. Therefore, the unchecked growth of the average laser power shown in Figure 1 promises a continuous and strong increase of the achievable productivity. Unfortunately, this simple scalability is compromised by physical constraints which impact the efficiency and the quality of the processing results. These constraints result from the physical material properties, from processing parameters, from the processing system, and last but not least from legal regulations due to the potential emission of soft X-rays.

Using the example of ablative processes on metals, some of these restrictions and possible remedies are considered in the following. We discuss which boundary

conditions challenge the realization of productive ultrafast laser processing and convey an extended but not complete list of nine (I.–IX.) conditions which have to be met for successful and highly productive ultrafast laser processing.

## 2 Influence of physical material properties

An important feature of ultrafast laser processing is that materials can be processed without creating a significant amount of melt which yields a superior “thermal precision” and is achieved by more or less directly sublimating the material. Since the latent heat of evaporation is significantly higher than the latent heat of melting, the ablation of material predominantly in its vaporous form according to (1) also requires a correspondingly elevated average power. In case of metals, the total volume-specific energy for evaporation is in the range of  $h_V \approx 60 \text{ J/mm}^3$  whereas it is only  $h_V \approx 10 \text{ J/mm}^3$  for melting. An approach to lower  $h_V$  might be taking benefit of thermal effects occurring with ultrashort pulses such as spallation [5] or Coulomb-explosions [6].

Furthermore, the energy penetration depth  $\ell_E$  during a single, ultrafast laser pulse into metals is of the order of a few tens of nanometers. This penetration of the deposited energy into the material can be approximated by an exponential law [7]. As extensively discussed by Neunschwander et al., e.g. in Ref. [8], with this approximation the ablation depth  $\ell_{abl}$  per laser pulse produced by a single pulse of a Gaussian beam is given by

$$\ell_{abl}(x, y) = \ell_E \cdot \left( \ln \left( \frac{2 \cdot A \cdot E_p}{h_V \cdot \ell_E \cdot \pi w_B^2} \right) - 2 \frac{x^2 + y^2}{w_B^2} \right) \quad (2)$$

where  $x$  and  $y$  are the cartesian coordinates,  $A$  is the absorptivity of the processed material,  $E_p$  is the pulse energy,  $w_B$  is the radius of the beam on the irradiated surface, and  $2E_p/\pi w_B^2 = \Phi_0$  is the peak fluence in the center of the beam. The product

$$h_V \cdot \ell_E = \Phi_{A,th} \quad (3)$$

describes the minimum amount of energy which has to be absorbed per unit area to generate ablation. The quantity  $\phi_{th} = \Phi_{A,th}/A$  is usually referred to as the ablation threshold fluence.

This energy penetration behavior has several consequences:

1. **Small ablation depth:** Even for fluences high above the ablation threshold, i.e., when  $\Phi_0 \gg h_V \cdot \ell_E$ , the

ablation depth for a single pulse is of the order of only a few hundred nanometers. On the one hand, this is favorable for very precise ablation, but on the other hand it also means that a large number of pulses needs to be applied on the same spot to remove a significant amount of material. The implication of this will be discussed further below.

**II. Optimum fluence for high productivity:** When the productivity, hence the volume ablation rate  $\dot{V}$  is calculated using the ablation depth given in Eq. (2), one finds [8]

$$\dot{V} = \frac{\pi w_B^2 \cdot \ell_E}{4} f_L \left( \ln \left( \frac{\phi_0}{\phi_{th}} \right) \right)^2 \quad (4)$$

As already stated in (1), this scales linearly with the average power  $P_{av} = f_L \cdot E_P$  when  $P_{av}$  is changed by increasing the pulse repetition rate  $f_L$ . When  $P_{av}$  is raised by increasing the pulse energy  $E_P$ , the ablation rate  $\dot{V}$  scales linearly with the average power only if the radius of the beam is adapted by  $w_B \propto \sqrt{E_P}$  to keep the fluence  $\phi_0$  constant.

Indeed, although the productivity given in (4) increases monotonously with increasing peak fluence, the process efficiency

$$\begin{aligned} \eta_P &= \frac{\dot{V} \cdot h_V}{P_{av}} = \frac{\pi w_B^2 \cdot \ell_E \cdot h_V}{4 \cdot E_P} \left( \ln \left( \frac{\phi_0}{\phi_{th}} \right) \right)^2 \\ &= \frac{A}{2} \frac{\phi_{th}}{\phi_0} \left( \ln \left( \frac{\phi_0}{\phi_{th}} \right) \right)^2 \end{aligned} \quad (5)$$

defined in (1) is also a function of the incident fluence and has a distinct maximum when the peak fluence in the center of the Gaussian beam amounts to  $\phi_{0,opt} = e^2 \cdot \phi_{th}$  [8, 9] (for a top-hat beam the optimum process efficiency  $\eta_P$  is reached with  $\phi_{0,opt} = e \cdot \phi_{th}$ ). With (1), (4), and (5) this means that in order to maximize the productivity

$$\dot{V} = \frac{\eta_P P_{av}}{h_V} = \frac{A}{2} \frac{\phi_{th}}{\phi_0} \left( \ln \left( \frac{\phi_0}{\phi_{th}} \right) \right)^2 \frac{P_{av}}{h_V}, \quad (6)$$

apart from increasing the average power one should also apply the optimum fluence to work with the maximum possible process (i.e. energetic) efficiency  $\eta_P$  by either choosing the optimum radius

$$w_{B,opt} = \sqrt{2E_P / (\pi \Phi_{0,opt})}, \quad (7)$$

of the laser beam on the surface, when the laser pulse energy  $E_P$  is given (typically the maximum pulse energy of the laser), or by choosing the optimum pulse energy

$$E_{P,opt} = \frac{1}{2} \cdot \pi \cdot w_B^2 \cdot \phi_{0,opt}, \quad (8)$$

when the radius of the laser beam is given (e.g. by the size of the envisaged structure). Both are very strict constraints on process design. High pulse energies allow for example to process large areas at the optimum fluence. If for some reason small laser spots are required, one possible solution is to distribute the pulse energy over many single spots with the correct pulse energy by spatially multiplexing the laser beam.

**III. Optimum fluence for good surface quality:** The quality of the processed surface strongly depends on the applied fluence. As described e.g. by Lauer et al. in Ref. [9], high-quality surfaces can only be generated at fluences below about 10x the ablation threshold. For a Gaussian beam this fortunately coincides with the fluence for maximum ablation efficiency.

**IV. Moderate process efficiency:** The maximum of the process efficiency obtained for Gaussian beams as given by Eq. (5) amounts to  $2A/e^2$ . Considering the absorptivity of about  $A \approx 40\%$  of radiation with a wavelength of 1  $\mu\text{m}$  in iron, one ends up with a maximum process efficiency in the order of 11%. This was experimentally confirmed by Lauer et al. in Ref. [9]. For comparison, in conventional laser fusion cutting the process efficiency is about 35%.

**V. Pulse energy requirements for deep structures:** The existence of an ablation threshold and the distinct optimum fluences also has an impact on creating structures such as holes or kerfs. During processing, the aspect ratio  $a$  (the depth of the structure divided by its width) increases with the number of applied pulses. The surface which is irradiated by the laser pulses is increasing about linearly with  $a$ . The fluence therefore decreases with processing time, reaching the ablation threshold at a certain depth of the structure. At this depth, the process becomes stochastic, as was directly observed during percussion drilling of Silicon by Döring et al. [10], and the quality of the structure is significantly decreased. The conditions for the quality limit of percussion drilling and the evolution of the hole depth was described in detail by Förster et al. [11] and Holder et al. [12], respectively. With minor modifications to the model introduced by [11], the maximum depth for percussion drilling with good quality and using a Gaussian beam can be approximated by

$$z_{max} \approx w_0 \cdot \sqrt{\frac{\left( \frac{\Phi_0 - \Phi_{th}}{A} \right)^2 - \Phi_{th}^2 \cdot \ln^2 \left( \frac{\Phi_0}{\Phi_{th}} \right)}{2 \cdot \Phi_{th}^2 \cdot \ln \left( \frac{\Phi_0}{\Phi_{th}} \right)}}. \quad (9)$$

Recently, it was shown by Feuer et al. [13] that the exits of percussion drilled, deep holes in stainless steel can only be achieved with very good quality, when the fluence reaching the hole exit is kept above about 2.8 times the threshold fluence. The consequence of this is that one either starts with a high fluence, where the process efficiency and the surface quality is low. Or one gradually increases the pulse energy during the process and starts at the optimum fluence with a reduced pulse energy first to ensure high process efficiency, with the consequence that the maximum average power of the laser is not exploited at the beginning of the process. Both constraints could in principle be circumvented by process parallelization, hence a simultaneous (beam splitting) or sequential (beam scanning) distribution of the laser power/energy on several holes that are drilled in parallel.

### 3 Influence of processing parameters

The preceding section outlined that several processing parameters are strictly defined by the application, the corresponding process and the material which is processed. Some of these constraints however also relate to the process strategy.

**VI. Heat accumulation:** The most important influence results from the very small ablation depth per pulse (see point 1. above). A large number of pulses on the same spot is usually required to achieve the desired total structure size. Unfortunately, a significant part  $\eta_{Heat}$  of the pulse energy stays inside the material as residual heat next to the interaction zone and only slowly diffuses into the surrounding material. With this the residual heat sums up from pulse to pulse. This heat accumulation effect leads to a steady increase of the temperature with increasing total number of laser pulses on the same spot. When a critical, total temperature increase  $\Delta T_{crit}$  is exceeded – usually to the melting temperature – the process changes completely and the benefit of ultrafast laser processing is lost. In the important case of three-dimensional heat flow, which typically applies when the surface of a rather large sample is processed within a small spot, the maximum average power  $P_L$ , which can be applied on a single spot to stay below the critical temperature increase  $\Delta T_{crit}$ , can be approximated with [14]

$$P_L \leq \frac{\Delta T_{crit}}{\sqrt{f_L}} \cdot \frac{\rho \cdot c_p}{5.2 \cdot \eta_{Heat}} \cdot \sqrt{\left(\frac{4 \cdot \pi \cdot k}{\rho \cdot c_p}\right)^3}, \quad (10)$$

where  $k$  is the heat conductivity,  $\rho$  the density, and  $c_p$  the specific heat capacity of the processed material. It is seen that, if  $\eta_{Heat}$  is minimized, e.g. by applying the optimum fluence discussed above, the limiting average laser power can only be increased by reducing the pulse repetition rate  $f_L$  of the laser. Heat accumulation between consecutive pulses can be avoided in a first approximation by moving the laser beam over the surface with a feed rate given by

$$v_F \approx 2 \cdot w_B \cdot f_L, \quad (11)$$

i.e. when only on single pulse hits each spot. As an example, for an ultrafast laser with a repetition rate of 10 MHz and focusing to a spot radius of 25  $\mu\text{m}$ , this means that a feed rate of 500 m/s is required to avoid heat accumulation. However, heat accumulation also results from multiple passes of the laser beam over the same location, again limiting the maximum average power, depending on the repetition rate  $f_p$  of the passes, which is defined by the feed rate and the length of the processed contour. Again, this limitation may be circumvented by process parallelization.

**VII. Air breakdown:** If for some reason the laser processing has to occur at fluences well above the ablation threshold, i.e. at high intensities, one has to consider the possibility of air breakdown, as visualized in Figure 2 (left), which starts at intensities of about  $>10^{13}$  W/cm<sup>2</sup> as e.g. described by Henn et al. [15] and Ireland et al. [16].

Figure 2 (right) shows an example for the limitation of the measured effective irradiance on the sample surface as a function of the calculated nominal irradiance due to air-breakdown. The effective irradiance was deduced from the diameter of the entrance of percussion-drilled holes in stainless steel. The holes were drilled with a Ti:Sapphire laser in “standard” laboratory ambient atmosphere at the wavelength of about 800 nm, a pulse duration of 1 ps and a focal length of 600 mm with a pulse energy of 5 mJ. The nominal irradiance was set by moving the focus from behind the sample up to the surface of the sample. It can be seen that air-breakdown has a huge effect on the focusing: Up to about  $10^{13}$  W/cm<sup>2</sup> the nominal and the effective irradiance are the same. Further increasing the nominal irradiance leads to a saturation of the effective irradiance with a maximum of about  $3 \cdot 10^{13}$  W/cm<sup>2</sup> and even decreasing with higher nominal irradiance.

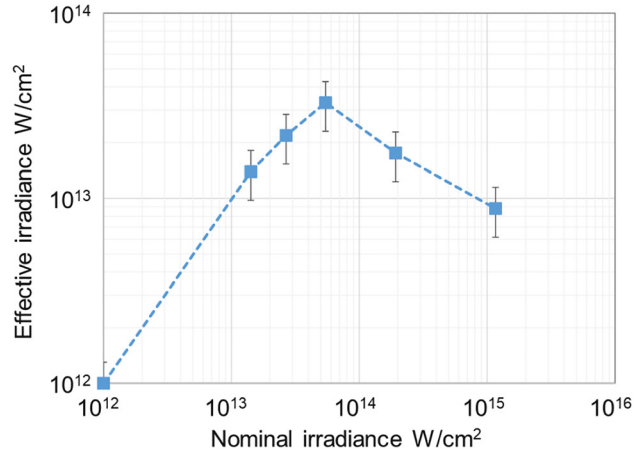
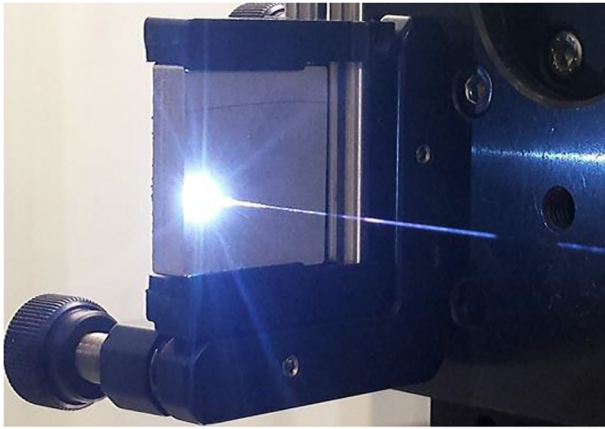


**Figure 2:** (Left) air-breakdown at high intensity; (right) limitation of the effective irradiance as a function of the nominal irradiance due to air-breakdown [15].

## 4 Influence of the processing system

The processing system itself and in particular the optical components can also severely influence the process. On the one hand, nonlinear effects in the processing optics caused by the ultrashort laser pulses can change the properties of the pulses such as the pulse duration or the spectrum. In the worst case, the high intensity inside the optical components may cause damage.

VIII. **Thermal focus shift:** On the other hand, small residual absorption of the transmitted laser power in the coatings and the bulk material heats up the material resulting in a temperature gradient from the center to the edge of the optical element. The temperature-dependence of the refractive index causes local distortion of the phase front of the transmitted laser beam. In first order this results in a thermal lens, usually with a positive refractive power. This lens causes a shift of the focus position. Normalized with the Rayleigh length  $z_R$ , the thermal focus shift can be expressed by

$$\frac{\Delta f}{z_R} \cong \frac{D^*}{\lambda \cdot M^2} \cdot P_{av} \quad (12)$$

where  $\lambda$  is the laser wavelength,  $M^2$  the beam quality factor, and  $D^*$  a lens-specific constant, which has to be determined experimentally. For new, AR-coated fused silica lenses  $D^*$  was found to be of the order of  $D^* \approx 0.5 \cdot 10^{-6} \text{ mm/W}$  by Faas et al. [17]. It is noted that lasers with low  $M^2$  and short wavelength induce a larger thermal focus shift. It is further noted that the focus shift increases linearly with the laser power. Assuming the 10 kW ultrafast

laser mentioned at the beginning and the  $D^*$  above, a focus shift of about four (!) Rayleigh lengths would clearly impede the process if no compensation is made.

## 5 Impact of legal regulations

Finally, it has to be noted that even legal regulations have strong impact on ultrafast laser processing.

IX. **X-ray emission:** X-ray measurements by Legall et al. [18] during materials processing with ultrafast lasers at a wavelength of  $1 \mu\text{m}$ , a pulse duration of 1 ps, an irradiance of about  $3 \cdot 10^{14} \text{ W/cm}^2$ , and an average power of 40 W yielded skin-dose rates  $\dot{H}$  (0.07) which exceed 100 mSv/h at the distance of 42 cm from the plasma, which is far above the legal annual limit. These high dose rates led to strict regulations for radiation protection, which involve a considerable additional effort for ultrafast materials processing.

Similar measurements and an analytical model calibrated with the experimental data was presented by Weber et al. [19]. Figure 3 shows the calculated dose rate at a distance of 50 cm from the plasma, normalized with the average laser power, as a function of the irradiance without (green line) and with shielding (dashed lines). It is noted that the dose rate is increasing linearly with the average laser power. The horizontal dashed red line represents the actual annual dose-limit for approval-free operation of ultrafast laser processing devices. This limit is exceeded at the above-mentioned parameters within 1 h when 1 W of average power is applied with a peak irradiance of about  $4 \cdot 10^{13} \text{ W/cm}^2$ .

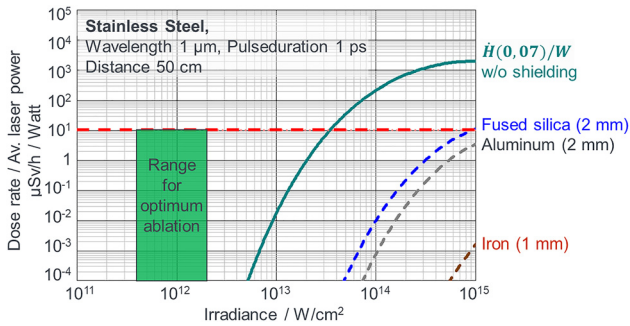


**Figure 3:** Dose rate at a distance of 50 cm from the plasma per average laser power as a function of the irradiance without (green line) and with shielding (dashed lines). The green rectangle marks the area of optimum processing regarding efficiency and quality.

However, as the spectrum of the X-ray emission is very soft, already shielding with fused silica and aluminum attenuates the radiation by at least four orders of magnitude when a peak irradiance of  $10^{14}$  W/cm<sup>2</sup> is applied, and still by more than two orders of magnitude for a peak irradiance of  $10^{15}$  W/cm<sup>2</sup> which is hardly of use for industrial applications. In any case it has however to be proven with rather elaborate measurements that this limiting dose rate is not exceeded anywhere outside of the processing system before the system can be cleared for operation.

The graph in Figure 3 is valid for processing of stainless steel where the ablation threshold is  $I_{th} \approx 2 \cdot 10^{11}$  W/cm<sup>2</sup>. The optimum irradiance for ultrafast processing with maximum efficiency and quality as described above is about 2x to 10x the ablation threshold and is marked with the green area in Figure 3 for reference. It is seen that this range is safe for average powers of up to at least 10 kW. Today, there are no indications that the values shown in Figure 3 can be significantly exceeded, also not by using burst-mode lasers as was recently published by Metzner et al. [20]. Nevertheless, there are still many open questions, and the topic is under investigation – meanwhile, the regulations apply.

## 6 Conclusions

In conclusion we have discussed an extended but not complete selection of nine (I.–IX.) distinct constraints for ultrafast laser materials processing and presented some approaches to overcome the limitations. It can be summarized that productive materials processing with ultrafast lasers is very demanding and that the scaling of the productivity requires innovative processing strategies such as simultaneous or sequential process parallelization.

When all the boundary conditions are considered correctly, successful applications become possible also exploiting high average laser powers. This was e.g. demonstrated by Holder et al. [21] where high-quality ablation of Silicon surfaces was achieved at average laser powers up to 1 kW reaching very high ablation rates of 230 mm<sup>3</sup>/min.

**Author contributions:** All the authors have accepted responsibility for the entire content of this submitted manuscript and approved submission.

**Research funding:** None declared.

**Conflict of interest statement:** The authors declare no conflicts of interest regarding this article.

## References

- [1] J. Negel, A. Voss, M. Abdou Ahmed, et al., “1.1 kW average output power from a thin-disk multipass amplifier for ultrashort laser pulses,” *Opt. Lett.*, vol. 38, no. 24, p. 5442, 2013.
- [2] T. Graf, “The laser: a universal tool for Industry 4.0,” in *Plenary Talk at the Proc. Laser pour l’Industrie (PLI) Conf., Parc des Expositions, Colmar, France, Club Laser et Procédés*, 2019.
- [3] T. Nubbemeyer, M. Kaumanns, M. Ueffing, et al., “1 kW, 200 mJ picosecond thin-disk laser system,” *Opt. Lett.*, vol. 42, no. 7, pp. 1381–1384, 2017.
- [4] M. Müller, C. Aleshire, A. Klenke, et al., “10.4 kW coherently combined ultrafast fibre laser,” *Opt. Lett.*, vol. 45, no. 11, p. 3083, 2020.
- [5] F. Vidal, T. W. Johnston, J.-C. Kieffer, and F. Martin, “Spallation induced by ultrashort laser pulses at critical tension,” *Phys. Rev. B*, vol. 70, 2004, Art no. 184125.
- [6] M. Hashida, H. Mishima, S. Tokita, and S. Sakabe, “Non-thermal ablation of expanded polytetrafluoroethylene with an intense femtosecond-pulse laser,” *Opt. Express*, vol. 17, no. 15, p. 13116, 2009.
- [7] S. Nolte, C. Momma, H. Jacobs, et al., “Ablation of metals by ultrashort laser pulses,” *J. Opt. Soc. Am. B*, vol. 14, no. 10, pp. 2716–2722, 1997.
- [8] B. Neuenschwander, G. F. Bucher, C. Nussbaum, et al., “Processing of metals and dielectric materials with ps-laserpulses: results, strategies, limitations and needs,” *Proc. SPIE*, vol. 7584, 2010, Art no. 75840R.
- [9] B. Lauer, B. Jäggi, and B. Neuenschwander, “Influence of the pulse duration onto the material removal rate and machining quality for different types of steel,” *Phys. Procedia*, vol. 56, pp. 963–972, 2014.
- [10] S. Döring, S. Richter, S. Nolte, and A. Tünnermann, “*In situ* imaging of hole shape evolution in ultrashort pulse laser drilling,” *Opt. Express*, vol. 18, pp. 20395–20400, 2010.
- [11] D. Förster, R. Weber, D. Holder, and T. Graf, “Estimation of the depth limit for percussion drilling with picosecond laser pulses,” *Opt. Express*, vol. 26, no. 9, pp. 11546–11552, 2018.
- [12] D. Holder, R. Weber, T. Graf, et al., “Analytical model for the depth progress of percussion drilling with ultrashort laser pulses,” *Appl. Phys. A*, vol. 127, p. 302, 2021.

- [13] A. Feuer, R. Weber, R. Feuer, D. Brinkmeier, and T. Graf, “High-quality percussion drilling with ultrashort laser pulses,” *Appl. Phys. A*, vol. 127, p. 665, 2021.
- [14] R. Weber, T. Graf, P. Berger, et al., “Heat accumulation during pulsed laser materials processing,” *Opt. Express*, vol. 22, no. 9, pp. 11312–11324, 2014.
- [15] M. Henn, G. Reichardt, R. Weber, T. Graf, and M. Liewald, “Dry metal forming using volatile lubricants injected into the forming tool through flow-optimized, laser-drilled microholes,” *JOM*, vol. 72, pp. 2517–2524, 2020.
- [16] C. L. M. Ireland and C. Grey Morgan, “Gas breakdown by a short laser pulse,” *J. Phys. D Appl. Phys.*, vol. 6, p. 720, 1973.
- [17] S. Faas, D. J. Foerster, R. Weber, and T. Graf, “Determination of the thermally induced focal shift of processing optics for ultrafast lasers with average powers of up to 525 W,” *Opt. Express*, vol. 26, no. 20, pp. 26020–26029, 2018.
- [18] H. Legall, C. Schwanke, S. Pentzien, G. Dittmar, J. Bonse, and J. Krüger, “X-ray emission as a potential hazard during ultrashort pulse laser material processing,” *Appl. Phys. A*, vol. 124, p. 407, 2018.
- [19] R. Weber, R. Giedl-Wagner, D. J. Förster, A. Pauli, T. Graf, and J. E. Balmer, “Expected X-ray dose rates resulting from industrial ultrafast laser applications,” *Appl. Phys. A*, vol. 125, p. 635, 2019.
- [20] D. Metzner, M. Olbrich, P. Lickschat, A. Horn, and S. Weißmantel, “X-ray generation by laser ablation using MHz to GHz pulse bursts,” *J. Laser Appl.*, vol. 33, 2021, Art no. 032014.
- [21] D. Holder, R. Weber, C. Röcker, et al., “High-quality high-throughput silicon laser milling using a 1 kW sub-picosecond laser,” *Opt. Lett.*, vol. 46, pp. 384–387, 2021.

## Bionotes



**Rudolf Weber**  
 Institut für Strahlwerkzeuge, Universität  
 Stuttgart, Pfaffenwaldring 43, D-70569  
 Stuttgart, Germany  
[rudolf.weber@ifsw.uni-stuttgart.de](mailto:rudolf.weber@ifsw.uni-stuttgart.de)

Rudolf Weber received his PhD in 1988 at the Institute of Applied Physics (IAP) of the University of Bern on the subject of “X-ray emission from laser-generated plasmas”. In the following years he

headed the research groups “Diode-Pumped Solid-State Lasers” and “Laser Material Processing” at the IAP. He then moved to industry, where he became managing director of engineering companies that developed laser sources and laser systems. Since 2008, he is lecturer at the University of Stuttgart and head of the process development group at the Institut für Strahlwerkzeuge (IFSW). In 2017 he habilitated on the topic “Process parameters for industrial laser applications and their impact on plant engineering” and is now an apl. Professor. His current work focuses on the theoretical and experimental basics of laser processes including X-ray emission from usp-processes, structuring of surfaces, and drilling of deep microholes with high-energy ultra-short pulsed lasers.



**Thomas Graf**  
 Institut für Strahlwerkzeuge, Universität  
 Stuttgart, Pfaffenwaldring 43, D-70569  
 Stuttgart, Germany

Thomas Graf was born in Switzerland in 1966. He received the physics M.Sc. degree in 1993 and the Ph.D. degree in 1996 from the University of Bern. After 15 months of research at Strathclyde University in Glasgow (UK) he was appointed head of the High-Power Lasers Group at the Institute of Applied Physics at the University of Bern in April 1999 where he was awarded the *venia docendi* in 2001 and appointed assistant professor in April 2002. In June 2004 he was appointed university professor and director of the Institut fuer Strahlwerkzeuge (IFSW) at the University of Stuttgart (D). At the IFSW Prof. Graf is engaged in research on high-power lasers, laser system engineering, and laser applications in manufacturing. At the University of Stuttgart Prof. Graf was vice dean of the faculty of Engineering Design, Production Engineering and Automotive Engineering from October 2010 to February 2013 and served as vice rector for Knowledge and Technology Transfer from February 2013 to September 2018. From 2001 to 2007 Prof. Graf served as a board member of the Swiss Society for Optics and Microscopy (SSOM), from 2008 to 2012 he was a board member of the European Optical Society (EOS), he is a board member of Photonics BW e.V., since 2016 as its chair, and is a member of the German Wissenschaftliche Gesellschaft Lasertechnik e.V., WLT, since 2013 member of its board as vice president Engineering Sciences. From 2009 to 2020 he was a member (as from April 2014 the chairman) of the supervisory board of the TLB GmbH.